(3 + 1)-dimensional crystal and antiferromagnetic structures in CeRuSn

Fast Track Communication

(3 + 1)-dimensional crystal and antiferromagnetic structures in CeRuSn

K Prokeš[1], **V Petříček**[2], **E Ressouche**[3], **S Hartwig**[1], **B Ouladdiaf**[4], **J A Mydosh**[5],
R-D Hoffmann[6], **Y-K Huang**[7] **and R Pöttgen**[6]

[1] Helmholtz–Zentrum Berlin für Materialien und Energie, Hahn-Meitner Platz 1, M-AQM, D-14109 Berlin, Germany

[2] Institute of Physics, ASCR v.v.i., Na Slovance 2, 182 21 Praha, Czech Republic

[3] SPSMS, UMR-E CEA/UJF-Grenoble 1, INAC, Grenoble, F-38054, France

[4] Institut Laue–Langevin, F-38042 Grenoble Cedex, France

[5] Kamerlingh Onnes Laboratory, Leiden University, 2300 RA Leiden, The Netherlands

[6] Institut für Anorganische und Analytische Chemie, Westfälische-Wilhelms-Universität Münster, D-48149 Münster, Germany

[7] Van der Waals-Zeeman Institute, University of Amsterdam, 1018XE Amsterdam, The Netherlands

E-mail: prokes@helmholtz-berlin.de

Abstract

At 320 K, the crystal structure of CeRuSn is commensurate with the related CeCoAl-type of structure by the doubling of the c lattice parameter. However, with lowering the temperature it becomes incommensurate with x and z position parameters at all three elemental sites being modulated as one moves along the c-axis. The resulting crystal structure can be conveniently described within the superspace formalism in (3 + 1) dimensions. The modulation vector, after initially strong temperature dependence, approaches a value close to $q_{nuc} = (0\ 0\ 0.35)$. Below $T_N = 2.8\ (1)$ K, CeRuSn orders antiferromagnetically with a propagation vector $q_{mag} = (0\ 0\ 0.175)$, i.e. with the magnetic unit cell doubled along the c-axis direction with respect to the incommensurate crystal structure. Ce moments appear to be nearly collinear, confined to the a–c plane, forming ferromagnetically coupled pairs. Their magnitudes are modulated between 0.11 and 0.95 μ_B as one moves along the c-axis.

Keywords: CeRuSn, incommensurate crystal structure, AF order, neutron diffraction, phase transition

S Online supplementary data available from stacks.iop.org/JPhysCM/26/122201/mmedia

(Some figures may appear in colour only in the online journal)

1. Introduction

The increasing number of compounds [1–3] having aperiodic (incommensurate) structures demonstrate that a standard scheme using a 3D lattice and unit-cell description is insufficient and a more general superspace-symmetry formalism [4] must be used. Incommensurate periodicities introduced by positional, occupational or charge modulations or by magnetic structure are then described in a similar way as in 3D space, however, extra dimensions are introduced. The simplest situation, in which atomic positions are incommensurately modulated around their average positions, thus leads to the introduction of one additional dimension. This more general approach offers a rigorous possibility to describe and solve incommensurate or other more complicated structures and to discover hidden symmetry relations [5]. We apply such a (3+1)-dimensional description to a unique intermetallic ternary compound CeRuSn.

CeRuSn adopts at room temperature a monoclinic crystal structure that is derived from the structure of CeCoAl

by a doubling along the *c*-axis [6–9] (denoted as the 2c structure). This leads to splitting of originally single Ce, Ru and Sn crystallographic positions into two inequivalent sites having different surroundings and different nearest neighbor distances. This led to predictions that Ce atoms are in different valence states, namely intermediate-valence $Ce^{(4-\delta)+}$ (at the Ce1 site) and trivalent Ce^{3+} (at the Ce2 sites) states [6, 8, 10]. Powder magnetic susceptibility behavior is compatible with only part of the Ce ions being in the Ce^{3+} state [7, 9, 10]. Moreover, it was shown that CeRuSn is close to magnetic instability and predicted that half of the Ce ions should develop magnetic moment and order antiferromagnetically (AF) [8]. Such an order has been recently identified below $T_N = 2.8$ K [7, 10, 11].

Below room temperature, a hysteretic phase transformation occurs on cooling between 290 and 160 K, leading to new superstructure Bragg reflections [7, 9, 12]. The 2c structure is reported to be replaced by various structural modifications, the dominant mode being a tripling of the basic CeCoAl cell (the 3c structure). Nevertheless, our recent synchrotron x-ray work showed that the 3c structure is only an approximation to the real crystal structure of CeRuSn [13]. However, neither of the literature sources could solve the details of the low-temperature crystal (and hence also the AF structure) unambiguously.

In this letter we report on the CeRuSn crystal and AF structures determined from neutron single crystal diffraction. Our finding disagrees with all previous results. We find that CeRuSn below room temperature exhibits an incommensurately modulated crystal structure that can be described in four dimensions using the superspace formalism [4]. The structure is related to the original CeCoAl type (we denote the CeCoAl type structure as the 1c structure) by a modulation vector of ≈0.35 along the *c*-axis [14]. The AF structure is described at low temperature also by an incommensurate propagation vector with respect to the 1c structure. However, it is commensurate with the low-temperature incommensurate crystal structure, having the magnetic unit cell doubled along the *c*-axis. Ce moments appear to be nearly collinear, confined to the *a*–*c* plane, forming ferromagnetic (F) pairs. Their magnitudes are modulated with a maximum of 0.95(8) μ_B as one moves along the *c*-axis. The shift of the atoms from their original positions is correlated with the modulation of Ce magnetic moments, however, these shifts are not due to the magnetic order as the AF order appears at temperature that is two orders of magnitude lower than the structural transition. The most surprising result is that the largest Ce moments are found for regions with the shortest Ce-ligand interatomic distances.

2. Experimental details

A large single crystal has been grown by means of a modified tri-arc Czochralski technique from a stoichiometric melt of the constituent elements. The quality of the crystal has been checked by the x-ray Laue backscattering. Magnetization curves $M(T)$ and the static magnetic susceptibility $\chi = M/H$, where H denotes the applied magnetic field along principal directions were measured in the temperature range between 1.8

and 350 K using the quantum design 14T physical properties measurements system (PPMS).

Neutron diffraction experiments were performed on the E4 diffractometer at the Helmholtz–Zentrum Berlin and CY-CLOPS and the D23 diffractometer at the Institut Laue–Langevin using a standard cryostat. To prevent effects of stress during thermal cycling, the sample was wrapped in all cases in an aluminum foil with its *b*-axis vertical. This geometry restricts the number of observable (*hkl*) reflections with respect to the *k* index, however, as it is shown below, the strongest magnetic reflections are situated within the *a*–*c* plane.

For refinement purposes we have collected on D23 several sets of diffraction data that included nuclear (both commensurate and incommensurate) and magnetic Bragg reflections. All the data were properly scaled and corrected for detector efficiency and geometrical factors to derive structure factors. Above room temperature we have fitted our data using the computer code FULLPROF [15] to the average 2c crystal structure and arrived at a very good agreement with literature sources [6, 9]. For the nuclear and magnetic data sets collected at low temperatures we have used the computer code Jana2006 [16], mainly developed by one of us (V.P.) that allows for treatment of incommensurate crystallographic and magnetic structures simultaneously, using the superspace formalism.

3. Results

3.1. Magnetic bulk measurements

The inverse magnetic susceptibility measured on a CeRuSn single crystal that is shown in figure 1(a) exhibits a significant anisotropy (the *c*-axis being the easy and the *b*-axis the hard magnetization direction) and hysteretic behavior between ~190 and ~300 K for all three principal directions similar to the thermal expansion and electrical resistivity [9]. Outside this hysteretic region the susceptibility follows a modified Curie–Weiss law, however, with different parameters. As an example, we show in figure 1(a) by red lines the best fits to the *c*-axis magnetic susceptibility. While above the hysteretic region we find an effective moment between 2.0 and 2.2 μ_B for the three principal directions, below the transition the effective moment is reduced. The change is, however, smaller than published for powder data [10, 7]. For the easy magnetization *c*-axis direction we find $\theta_p = -16.6(2)$ K, suggesting predominant AF exchange interactions in CeRuSn.

In the inset of figure 1(a) we show the low-temperature portion of the CeRuSn magnetic susceptibility $\chi(T)$ measured in a field of 0.1 T applied along the *c*-axis. The maximum in the $d(\chi(T) * T)/dT$ (marked by arrow) that indicates the magnetic phase transition to the magnetic state in the case of antiferromagnets [17] appears at the very same temperature of 2.78(5) K as reported previously [7, 10, 11]. This value shifts with increasing applied fields to lower temperatures suggesting an AF order in CeRuSn. Magnetization curve obtained for CeRuSn at 2 K is shown in figure 1(b). After the initial fast increase, the Ce moment slowly saturates to 0.69(1) μ_B/Ce in 14 T for the *c*-axis direction. For the *a* and *b*-axis directions, no saturation is observed even in fields of 14 T.
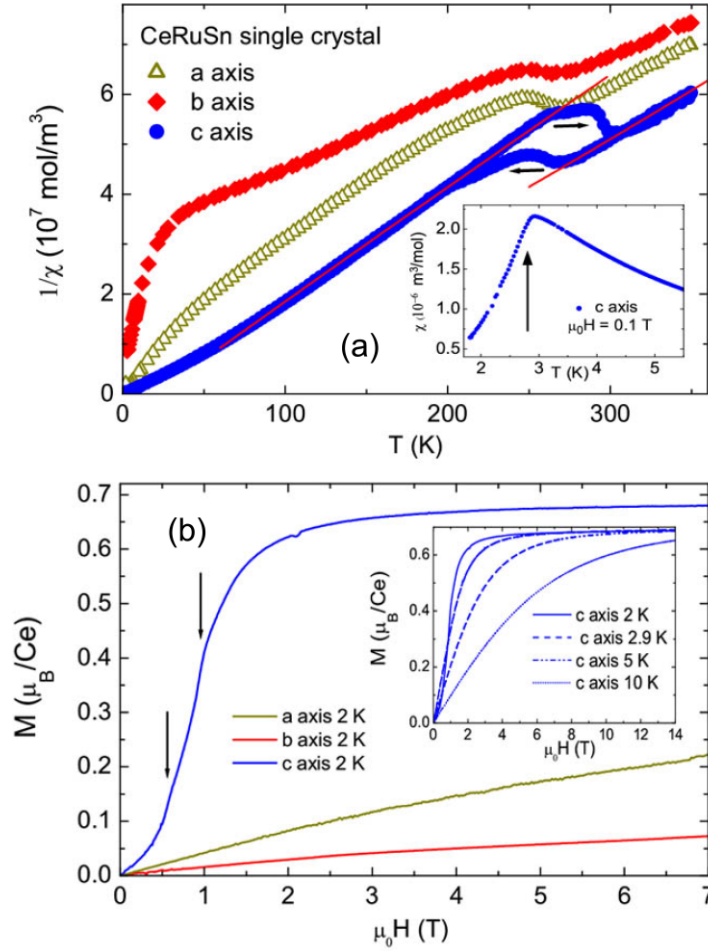
Figure 1. Temperature dependence of the inverse magnetic susceptibility $1/\chi(T)$ measured in a field of 1 T applied along the CeRuSn principal directions with decreasing temperature (a). For the c-axis direction also the warming branch is shown. Solid lines represent best fits to modified Curie–Weiss laws. The low-temperature portion of $\chi(T)$ measured in a field of 0.1 T along the c-axis is shown in the inset. The arrow marks the Néel temperature. In panel (b) the magnetic field dependence of magnetization measured at 2 K along the principal directions is shown. The arrow marks metamagnetic transitions. In the inset magnetization curves along the c-axis direction measured at several temperatures are shown.

The field derivative of the c-axis magnetization curve exhibits two clearly visible maxima at 0.55 and 0.93 T (marked in figure 1(b) by arrows) that are due to a domain-repopulation effect and/or moment-reorientation towards finally F alignment. For the c-axis direction we show in the inset of figure 1(b) further magnetization curves at selected temperatures. As the temperature increases, the character of the magnetization process changes and no AF–F transition can be discerned above T_N. For this orientation we find a significant increase and saturation of the magnetization even at temperatures that are much higher than T_N.

3.2. Crystal structure

In figure 2(a) we show a complete neutron Laue diffractogram obtained at CYCLOPS at 1.8 K with incident beam approximately along the a-axis. The b-axis is vertical. A clear splitting of some structural reflections upon cooling is demonstrated in panel figures 2(b)–(d). It appears that all split reflections (hkl) can be indexed with a propagation vector of the type $q_{nuc} = (00q)$, with q depending on temperature. As the temperature

is lowered, the type of the q_{nuc} remains, however, the q value changes and eventually stabilizes below ≈ 150 K. Below T_N yet more reflections appear that are assigned to a magnetic origin that are also indexable with a similar type of propagation vector. Relevant representative regions taken at 10 K and at 1.8 K are shown in figures 2(e) and (f), respectively as well.

In figure 3(a) a false color-coded temperature dependence of a reciprocal scans of CeRuSn along the [0 0 l] direction upon warming up between 10 and 320 K is shown. At low temperature one observes clearly two Bragg reflections centered at (0 0 $\approx$0.35) and (0 0 $\approx$0.65) incommensurate positions. As the temperature increases the two incommensurate super-structure reflections get closer and merge above 290 K to a commensurate value $q = 1/2$. Upon cooling the same tendency is seen, however, the (0 0 1/2) commensurate reflection splits at lower temperature exhibiting an appreciable hysteresis. Fitted positions and intensities of both the commensurate (0 0 1/2) and the lowest-q incommensurate reflection are shown in figures 3(b) and (c), respectively. The commensurate reflection loses intensity upon cooling and saturates below 180 K at
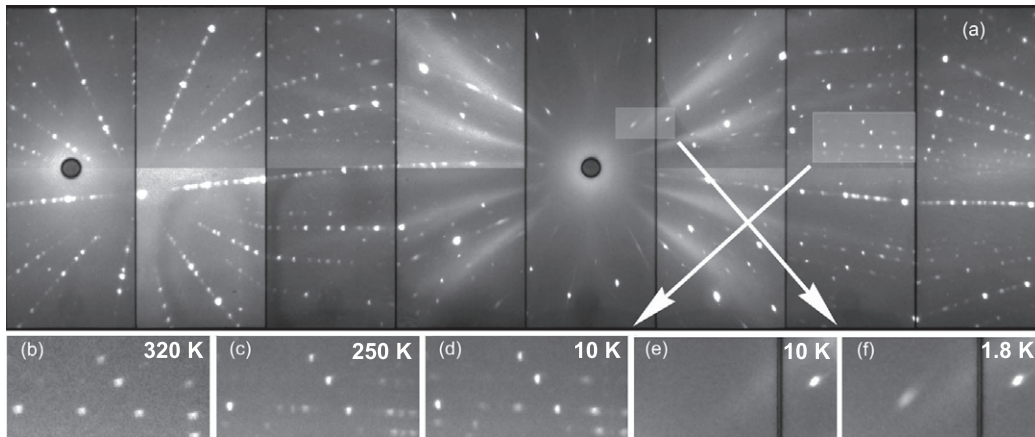
Figure 2. Neutron Laue diffraction pattern of CeRuSn taken at 1.8 K (a) with incident beam approximately along the *a*-axis (a). The *b*-axis is vertical. The temperature development of a small highlighted region showing the splitting of some structural $(hkl + 0.5)_{1c}$ reflections is demonstrated in panels (b)–(d). A region, in which magnetic reflections appear below T_N is highlighted in panels (e) and (f), respectively.
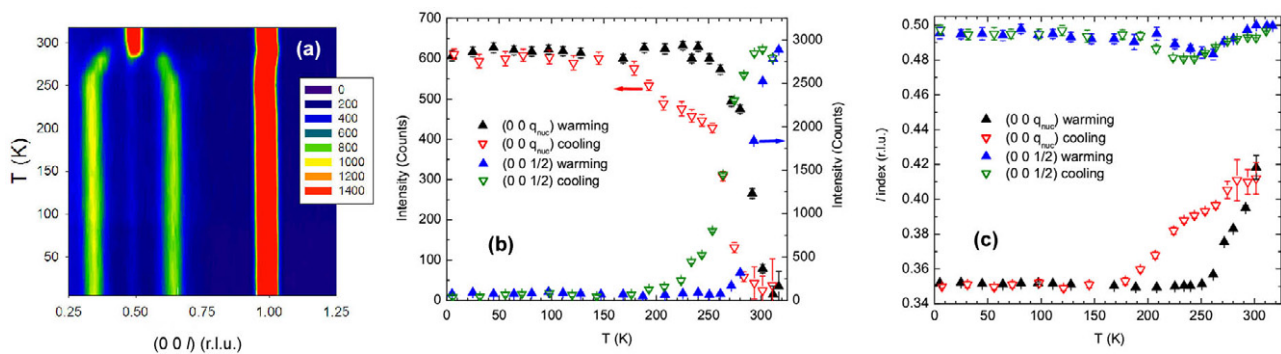
Figure 3. A color-coded temperature dependence of CeRuSn reciprocal scans taken along the [0 0 *l*] direction (a) upon warming up between 10 and 320 K. Fitted reflection intensities and positions are shown in panels (b) and (c), respectively.

a small constant but nonzero intensity. With increasing the temperature it gains the same intensity as before, however, at higher temperature. The incommensurate reflections show the opposite temperature dependence. The (001) reflection decreases in intensity by a few percent across the transition, showing the same hysteresis. Scans from the E4 instrument (not presented) show very similar results. Reciprocal scans on E4 with the best possible resolution showed that it is not possible to split incommensurate superstructure reflections (that are broader than commensurate ones) into individual components. This suggests that we deal with an incommensurate crystal structure described within the four-dimensional space by a single modulation.

3.3. Antiferromagnetic structure

Using the commensurate nuclear reflections collected at 320 K, we have confirmed that the CeRuSn crystal structure conforms with the 2c structure as published in literature [6, 7, 9]. In the case of the low-temperature refinement we included both the commensurate and incommensurate reflections simultaneously. Initial parameters for the modulated part were taken from laboratory x-ray single crystal experiments that will be reported elsewhere [14]. It appeared that the incommensurability at low temperatures can be facilitated only by assuming that

the *x* and *z* positional parameters of all the atoms are modulated as one moves along the *c*-axis. A schematic representation of the CeRuSn crystal structure at low temperatures together with numerical results is given in supplementary material[8].

In figure 4(a), a color-coded temperature dependence of CeRuSn reciprocal scans taken along the [1 0 *l*] direction upon warming up between 1.4 and 3.1 K is shown. All observed magnetic reflections can be indexed using a propagation vector $q_{mag} = (0\ 0 \approx 0.175)$. Fitted temperature dependence of the $(1\ 0\ -q_{mag})$ reflection intensity $I(T)$ together with the best fit to the empirical formula $I(T) = I_{T=0}(1 - \frac{T}{T_N})^{2\beta}$ [18] used above 2.0 K are shown in figure 4(b). The derived magnetic phase transition temperature $T_N = 2.89(5)$ K agrees very well with magnetic bulk measurements. The inset of figure 4(b) show the temperature dependence of the propagation vector that is found to decrease somewhat with increasing the temperature. In the low-temperature limit, the magnetic propagation vector is half of the propagation vector describing the incommensurate crystal structure, i.e. $q_{mag} = q_{nuc}/2$ suggesting that the AF unit cell is twice as large with respect to the incommensurate crystal structure
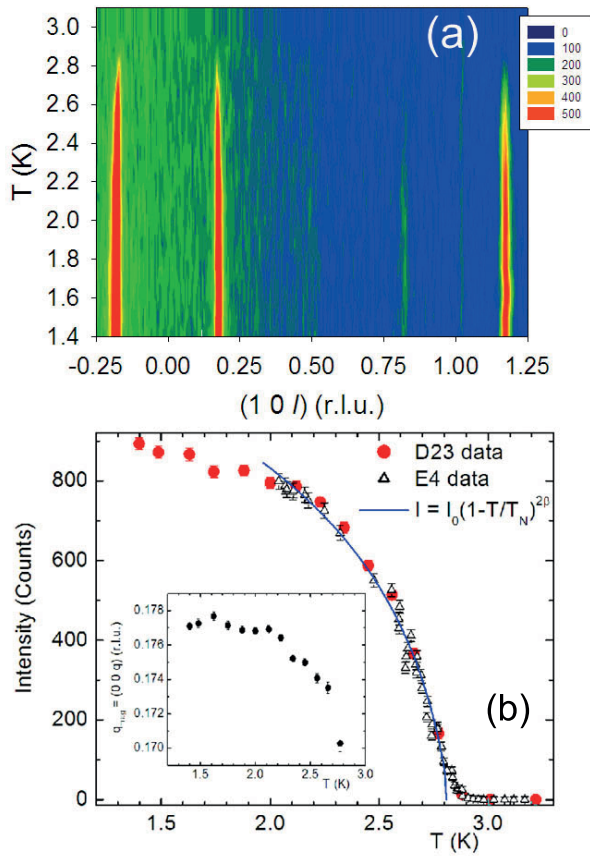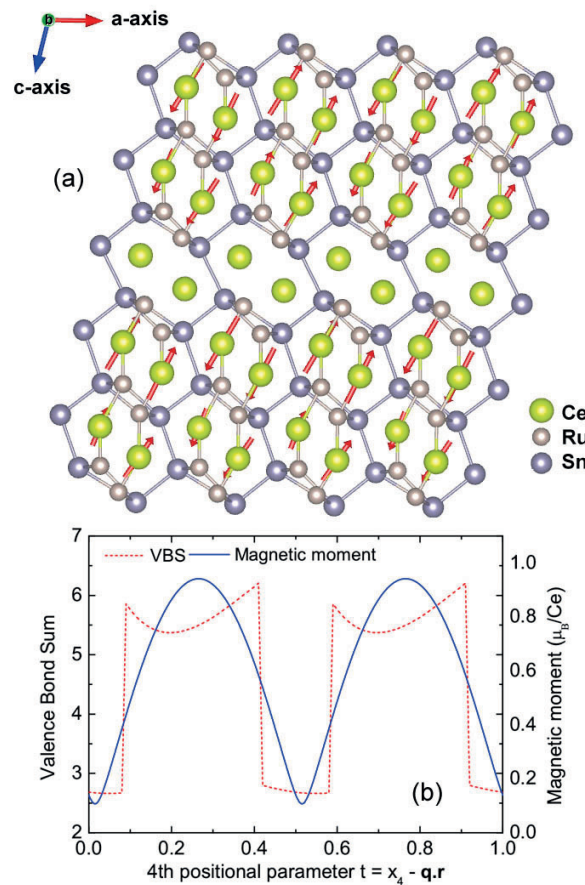
Figure 4. Temperature dependence of CeRuSn reciprocal [1 0 *l*] scans (a) taken upon warming up between 1.4 and 3.1 K. Fitted temperature dependence of reflection intensities together with the best fit to the given empirical formula are shown in panel (b).

Figure 5. A schematic representation of the CeRuSn AF structure, projected onto the *a*–*c* plane. $2a \times 1b \times 5c$ crystallographic unit cells corresponding to the undistorted crystal structure of the CeCoAl type are shown. Magnetic moments are represented by arrows. Ce moments are modulated along the *c*-axis, and the Ce–Ce and the shortest Ce–Ru interatomic distances are shown by bonds. Panel (b) shows the correspondence between the magnetic moment magnitude and the bond valence sum, both as a function of the internal 4th positional parameter *t*.

modulation. For observed magnetic reflections clear extinction rules exist leading to several possible superstructure space groups [4, 19]. A schematic representation of the CeRuSn reciprocal $k = 0$ plane including extinction rules is given in supplementary material (available at stacks.iop.org/JPhysCM/26/122201/mmedia) (see footnote 8).

After checking all the possible symmetries it became clear that the relevant superspace group is $C2/m \cdot 1'(\alpha 0 \gamma)0ss$. The best fit of the observed data leads to the AF structure depicted in figure 5(a). Ce magnetic moments appear to be nearly collinear, confined to the *a*–*c* plane, forming F coupled pairs that are reverted within the same unit cell in the *a*-axis direction. Yet, the non-collinearity of Ce moments is significant. Attempts to keep them collinear lead to worse agreements. The Ce moment magnitudes varies between 0.11 and 0.95 μ_B as one moves along the *c*-axis.

4. Discussion and conclusions

Our findings are in many respects similar to results obtained from previous powder neutron diffraction experiments [7]. The powder work, however, led to the conclusion that the AF structure is cycloidal. The disagreement can be explained by small intensities of superstructure and magnetic reflections involved and the Rietveld type refinement of powder data. The average

moment from the single crystal work amounts to 0.61(6)μ_B, which is a somewhat smaller value with respect to the magnetic bulk measurements that led to a value of 0.69(1) μ_B.

As it is shown in figure 5(b), Ce moments are not modulated by a simple sine wave and a very clear relation between the moment magnitude and interatomic distances exists. To document this, we have calculated the Ce bond valence sums (BVS) that express in a simplified way the valence state of the atom [20][9] and construct BVS as a function of the reduced internal 4th positional parameter *t* in the same manner as the positional dependence of the magnetic moment. Surprisingly, this relation has the opposite dependence to the expected one. The Ce magnetic moments appear to be the largest in regions where short Ce–Ru distances exist (and hence the largest BVS values). It has to be noted that this solution is very robust. The attempt to 'fix' large moments in areas with large Ce–Ru distances leads to an agreement

---

[9] As no tabulated values for parameters *b* and R_0 exist in the literature, we have used the values $b = 0.37$ and $R_0 = 3$ Å in the calculation.

factor that is at least by a factor of three worse. This finding is in direct disagreement with previous *ab initio* calculations by Matar *et al* that predicted a sizable moment only on Ce sites that have significantly larger distances to surrounding ligands. We note that the calculation has been performed for the high-temperature 2c phase. It remains to be shown whether the electronic structure of the incommensurately modulated CeRuSn at low temperatures is modified in such a way that stable and sizable Ce moments can exist in regions with very short interatomic distances.

In conclusion, we have shown that CeRuSn posses at low temperatures an incommensurate crystal structure with all atoms shifted from their average positions. The modulation vector $q_{nuc} = (0\ 0\ 0.35)$ is close but not equal to a commensurate 1/3 value suggesting that all previous studies are in error. Our single crystal diffraction work agrees well with recent laboratory x-ray studies [14] and, because our solution implies a wide distribution of interatomic distances, it is able also to explain recent synchrotron results [13]. Furthermore we have determined the AF structure that is commensurate with respect to the incommensurate crystal structure by doubling along the *c*-axis direction. We have shown that in order to describe both structures in an effective way and to gain valuable insights regarding the relation between the moment arrangement and the local atomic arrangements, it is beneficial to use superspace formalism within $(3 + 1)$ dimensions.

Acknowledgments

References

[1] Toudic B, Garcia P, Odin Ch, Rabiller Ph, Ecolivet C, Collet E, Bourges Ph, McIntyre G J, Hollingsworth M D and Breczewski T 2008 *Science* **319** 69

Janssen T, Chapuis G and De Boissieu M 2007 *Aperiodic Crystals: From Modulated Phases to Quasicrystals* (Oxford: Oxford University Press) p 1

[2] Ling Ch D *et al* 2013 *J. Am. Chem. Soc.* **135** 6477

[3] Singh S, Nayak J, Rai A, Rajput P, Hill A H, Barman S R and Pandey D 2013 *J. Phys.: Condens. Matter* **25** 212203

[4] Perez-Mato J M, Ribeiro J L, Petříček V and Aroyo M I 2012 *J. Phys.: Condens. Matter* **24** 163201

[5] Urcelay-Olabarria I, Perez-Mato J M, Ribeiro J L, Garcia-Munoz J L, Ressouche E, Skumryev V and Mukhin A A 2013 *Phys. Rev. B* **87** 014419

[6] Riecken J F, Hermes W, Chevalier B, Hoffmann R-D, Schappacher F M and Pöttgen R 2007 *Z. Anorg. Allg. Chem.* **633** 1094

[7] Prokeš K, Mydosh J A, Prokhnenko O, Stein W-D, Landsgesell S, Hermes W, Feyerherm R and Pöttgen R 2013 *Phys. Rev. B* **87** 094421

[8] Matar S F, Riecken J F, Chevalier B, Pöttgen R, Al Alam A F and Eyert V 2007 *Phys. Rev. B* **76** 174434

[9] Fikáček J, Prokleška J, Míšek M, Custers J, Daniš S, Prchal J, Sechovský V and Císařová I 2012 *Phys. Rev. B* **86** 054108

[10] Mydosh J A, Strydom A M, Baenitz M, Chevalier B, Hermes W and Pöttgen R 2011 *Phys. Rev. B* **83** 054411

[11] Fikáček J, Prokleška J, Prchal J, Custers J, Sechovský V and Císařová I 2013 *J. Phys.: Condens. Matter* **25** 416006

[12] Feyerherm R, Dudzik E, Valencia S, Mydosh J A, Huang Y-K, Hermes W and Pöttgen R 2012 *Phys. Rev. B* **85** 085120

[13] Prokeš K, Kimber S A J, Mydosh J A and Pöttgen R 2014 *Phys. Rev. B* at press

[14] Hoffmann R-D, Prokeš K, Mydosh J A and Pöttgen R 2014 in preparation

[15] Roisnel T and Rodriguez-Carvajal J 2001 *Mater. Sci. Forum* **378** 118

[16] Petříček V, Dušek M and Palatinus L 2006 *The Crystallographic Computing System* (Praha: Institute of Physics)

[17] Fisher M E 1962 *Phil. Mag.* **7** 1731

[18] Birgeneau R J, Skalyo J and Shirane G 1970 *J. Appl. Phys.* **41** 1303

[19] Janssen T, Janner A, Looijenga-Vos A and de Wolf P M 2006 *International Tables for Crystallography* vol C (Amsterdam: Kluwer) p 899

[20] Brown I D and Altermatt D 1985 *Acta Crystallogr.* **B41** 244